



Blue light generation by frequency doubling a diode laser
by Xiaoguang Sun

A dissertation submitted in partial fulfillment of the requirements for the degree of Doctor of
Philosophy in Physics
Montana State University
© Copyright by Xiaoguang Sun (2001)

Abstract:

In this dissertation, we present a simple scheme for construction of a low noise continuous wave blue light source by frequency doubling a Fabry-Perot diode laser in a potassium niobate crystal inside a bow tie ring cavity. By feeding back the ring cavity transmission into the diode laser after reflection off a grating, the diode laser operates in single mode and is frequency locked to the cavity resonance. Using a simple analytic form of the beam parameters for the ring cavity, the optimum cavity configuration is found for a high degree of mode matching between the diode laser output beam and the ring cavity. The wavelength of the blue output is tunable from 484-488nm, has a narrow linewidth of 1.25MHz, and has a continuous tuning range of more than 10GHz. The output power of the blue light is 18mW with intensity fluctuations less than 0.02dB. The blue light is a near diffraction limited Gaussian TEM₀₀ mode with $M^2 \approx 1$. Numerical simulation of the SHG is carried out by using the Fourier space method, and the experimental results are in good agreement with the simulation.

BLUE LIGHT GENERATION BY FREQUENCY DOUBLING

A DIODE LASER

by

Xiaoguang Sun

A dissertation submitted in partial fulfillment
of the requirements for the degree

of

Doctor of Philosophy

in

Physics

MONTANA STATE UNIVERSITY
Bozeman, Montana

June 2001

D378
Sec 699

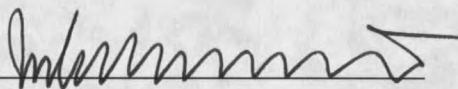
APPROVAL

of a dissertation submitted by

Xiaoguang Sun

This dissertation has been read by each member of the dissertation committee and has been found to be satisfactory regarding content, English usage, format, citations, bibliographic style, and consistency, and is ready for submission to the College of Graduate Studies.

Dr. John Carlsten

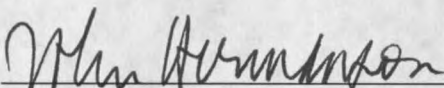

(Signature)

6-7-01

Date

Approved for the Department of Physics

Dr. John Hermanson

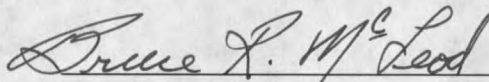

(Signature)

6-10-01

Date

Approved for the College of Graduate Studies

Dr. Bruce R. McLeod


(Signature)

7-1-01

Date

STATEMENT OF PERMISSION TO USE

In presenting this dissertation in partial fulfillment of the requirements for a doctoral degree at Montana State University, I agree that the Library shall make it available to borrowers under rules of the Library. I further agree that copying of this dissertation is allowable only for scholarly purposes, consistent with "fair use" as prescribed in the U.S. Copyright Law. Requests for extensive copying or reproduction of this dissertation should be referred to University Microfilms International, 300 North Zeeb Road, Ann Arbor Michigan 48106, to whom I have granted "the exclusive right to reproduce and distribute my dissertation in and from microform along with the non-exclusive right to reproduce and distribute my abstract in any format in whole or in part."

Signature  _____Date 06/11/2001

ACKNOWLEDGEMENTS

I would like to thank my advisor Dr. John Carlsten for giving me the opportunity to work in his lab on this project. I am grateful for his guidance, encouragement and support.

I would like to thank Kevin Repasky, Lei Meng, Sytil Murphy, Cheryl Berger and Pete Roos for reading my paper and dissertation, making good suggestions and correcting my English.

I would like to thank Norm Williams for his help with matching.

Finally, I would like to thank my family, especially my wife, for their support.

TABLE OF CONTENTS

1. INTRODUCTION.....	1
Nonlinear frequency conversion	2
Phase-matching	3
Continuous wave second harmonic generation	5
Overview of the dissertation	7
2. BOW TIE RING CAVITY DESIGN.....	9
Mode in a bow tie ring cavity.....	10
Stability region and mode spot size stability of the ring cavity	14
Mode with the crystal.....	15
Mode matching between the diode laser and the ring cavity	18
Cavity tuning for large frequency scanning range	23
3. SHG CALCULATION USING THE FOURIER-SPACE METHOD	25
Mathematical development	27
Numerical simulation of SHG in a KNbO ₃ crystal.....	30
Phase mismatching and SH power	34
Beam profile and the beam quality of the SH wave.....	39
Discussion and conclusion	44
4. CONSTRUCTION OF A BLUE LIGHT SOURCE BY SHG	46
Experimental setup and apparatus.....	47
Passive locking.....	50
Experimental results.....	53
The second experiment.....	64
5. SUMMARY	68

REFERENCES.....	69
APPENDICES.....	74
APPEDIX A: Effective cavity distance with a tilted crystal.....	75
APPEDIX B: Plane wave in anisotropic media	80
APPEDIX C: Potassium Niobate (KNBO ₃) crystal	87
APPEDIX D: Simulation programs	91

LIST OF TABLES

Table	Page
1.1 CW SHG Experiments	8

LIST OF FIGURES

Figure	Page
2.1. The bow tie ring cavity.....	9
2.2. The calculated beam waists in the ring cavity.....	13
2.3. The stability region of a bow tie ring cavity.	14
2.4. The beam waist location with the position of the crystal between the two curved mirrors.	17
2.5. Focus the diode laser output by two spherical lenses.....	19
2.6. The solution for the large beam waist size with an ellipticity of 1:2.7, and the small beam is circular with different incident angle.	21
2.7. Cavity tuning of a bow tie ring cavity.....	23
3.1. The input fundamental wave and the nonlinear crystal.	31
3.2. Conversion efficiency of the calculated and theory of a plane wave model.....	33
3.3. Illustration of why a positive phase mismatching is needed for maximum conversion of focused Gaussian beams.	34
3.4. The beam waists of the SH wave inside the crystal and the peak positions of the fundamental and SH wave inside the crystal.....	35
3.5. The optimum phase mismatching Δk vs. input beam waist size and the normalized SH power with phase mismatching.	36
3.6. The SH power vs. input beam waist size.	38
3.7. SH power vs. beam waist location of the fundamental wave.....	39
3.8. Far-field pattern of the SH wave.	40
3.9. The M^2 parameters of the SH wave for different input beam waist sizes	42
3.10. The effective beam waist sizes and the astigmatism of the SH wave....	43
3.11. The profiles of the SH beams at the focus.	44

4.1	Experimental setup.....	47
4.2	The spectrum of the laser diode.....	53
4.3	The beam profile of the cavity transmissions.....	55
4.4	The blue light generated vs. the pump power inside the cavity.....	57
4.5	The output blue light power fluctuation and the relative intensity noise (RIN) of the blue light.....	58
4.6	Beam waists of the horizontal and vertical plane with change of axial position z and the beam profile of the output blue.....	60
4.7	The single-sided frequency noise power spectrum of the blue light and the calculated field spectrum.....	62
4.8	Measured frequency ramping of the fundament light by a wavemeter.....	63
4.9	The setup for the second experiment.....	64
4.10	Far-field beam profile of the blue light.....	65
4.11	The real beam path and the designed beam path.....	67
A.1	The effective length of the crystal at normal incidence.....	76
A.2	The effective distance for the horizontal plane and the vertical plane.....	77
A.3	The effective distance between the two curved mirrors.....	79
B.1	The two eigenmodes determined by the index ellipsoid.....	82
B.2	Relations of \vec{S} , \vec{k} , \vec{D} , \vec{E} and \vec{H}	83
B.3	Gaussian beam propagation in a uniaxial crystal.....	85
C.1	The crystal coordinate system of the KNbO ₃ crystal.....	88
C.2	The phase matching condition at 968nm-976nm.....	90
C.3	Coordinate system of the simulation and the crystal principle axes.....	90

ABSTRACT

In this dissertation, we present a simple scheme for construction of a low noise continuous wave blue light source by frequency doubling a Fabry-Perot diode laser in a potassium niobate crystal inside a bow tie ring cavity. By feeding back the ring cavity transmission into the diode laser after reflection off a grating, the diode laser operates in single mode and is frequency locked to the cavity resonance. Using a simple analytic form of the beam parameters for the ring cavity, the optimum cavity configuration is found for a high degree of mode matching between the diode laser output beam and the ring cavity. The wavelength of the blue output is tunable from 484-488nm, has a narrow linewidth of 1.25MHz, and has a continuous tuning range of more than 10GHz. The output power of the blue light is 18mW with intensity fluctuations less than 0.02dB. The blue light is a near diffraction limited Gaussian TEM₀₀ mode with $M^2 \approx 1$. Numerical simulation of the SHG is carried out by using the Fourier space method, and the experimental results are in good agreement with the simulation.

CHAPTER-1

INTRODUCTION

Existing laser sources, such as semiconductor lasers, gas lasers, dye lasers and solid-state lasers, cover a wide range wavelengths. But many practical demands from physical, chemical and biophysical research, medical diagnostics and therapies, and environmental monitoring, require tunable coherent light sources in new spectral regions not accessible to these lasers. Examples include lithography and grating writing in the deep ultraviolet (UV) region, data storage and color display in the blue region, and ranging and pollutant detection in the infrared region. Thus it is a matter of practical importance to widen the range of wavelengths generated by the existing laser sources. For these applications, the desired features of the light sources usually include: high power, single frequency operation, narrow linewidth, low noise, good beam quality, tunability, compactness, low cost, diode pumping, all-solid-state construction for easy maintenance, and often continuous wave (CW) operation.

Significant progress has been made in the development of nonlinear optical materials for frequency conversion in recent years; a variety of new crystals with large nonlinear coefficients, large size and good optical quality are commercially available. Light sources based on nonlinear frequency conversion using these nonlinear materials to generate the desired wavelength have become practical and can meet those requirements, and even are replacing some of the existing gas lasers that are inefficient and large.

In addition, using nonlinear frequency conversion can also generate squeezed light. Squeezed state of light is a nonclassical state for which the variation in one of the two quadrature-phase amplitudes of the electromagnetic field is less than that of the vacuum state of the field. Therefore squeezed light is in some sense quieter than the light in the vacuum state and hence can be employed to improve measurement precision beyond the standard quantum limits¹.

Nonlinear frequency conversion

The basic principles of nonlinear frequency conversion are well known¹: when an electromagnetic field propagates through a medium, the polarization of the medium can be written as a power series of the input field E

$$P = \epsilon_0 \chi^{(1)} \cdot E + \epsilon_0 \chi^{(2)} \cdot E^2 + \epsilon_0 \chi^{(3)} \cdot E^3 + \dots \quad 1.1$$

where ϵ_0 is the electric permeability of vacuum, $\chi^{(1)}$, $\chi^{(2)}$ and $\chi^{(3)}$ are the linear, second order and third order susceptibility, and the corresponding terms are the linear, second and third order polarization, etc. As an example, suppose that if two light beams, one at frequency ω_1 and another at ω_2 , are propagating in the medium. The second order polarization can be written as:

$$P^{(2)} = \epsilon_0 \chi^{(2)} \left[\frac{1}{2} E_1 e^{-i\omega_1 t} + \frac{1}{2} E_2 e^{-i\omega_2 t} + cc \right]^2 \quad 1.2$$

We can see that the second order polarization will have frequencies at $2\omega_1$, $2\omega_2$, $\omega_1 - \omega_2$ and $\omega_1 + \omega_2$. Radiation at new frequencies will be generated. This second order term leads to the second harmonic generation (SHG), sum frequency generation,

difference frequency generation and optical parametric generation (OPG): The third order term produces frequency tripling, phase conjugation and four-wave mixing, etc.

The linear susceptibility $\chi^{(1)}$ is usually in the range of 1~10, $\chi^{(2)}$ in 10^{-12} ~ 10^{-10} m/V, and $\chi^{(3)}$ in 10^{-21} ~ 10^{-19} m²/V^{2.2}. To observe the nonlinear polarization, very intense light, such as that from a laser is required. Note that the absolute value of the second order susceptibility $\chi^{(2)}$ is about 9 orders of magnitude higher than that of the third order susceptibility $\chi^{(3)}$. Thus many of the practical nonlinear frequency conversion light sources are based on the second order effect, with the two most important categories being SHG and OPG.

Phase-matching

To observe a significant amount of generated light, phase matching is of vital importance. This can be explained as the following: inside the nonlinear medium, all of the induced polarization generated by the fundamental wave along its path will add coherently, and at the output of the medium, if all the waves are in phase, constructive interference will occur, and the maximum effect is achieved. On the contrary, if the phase of the generated wave adds destructively, the intensity will be diminished. A simple plane wave analysis of this nonlinear process will show that the power of the generated wave is¹:

$$P \propto \frac{\sin^2(\Delta kL/2)}{(\Delta kL/2)^2} \quad 1.3$$

where phase matching $\Delta k = k_1 + k_2 - k_3$ ($\omega = \omega_1 \pm \omega_2$), with k_1, k_2 being the wave vectors of the input waves, k_3 the generated wave, and L the length of the nonlinear medium. In general, because of the dispersion of the medium, the optical wave at different frequencies will propagate with different phase velocities, so $\Delta k \neq 0$.

One method to achieve phase matching is to utilize the birefringence of the anisotropic crystal. In the anisotropic medium, the index of refraction for a wave at a given frequency depends on the direction of propagation as well as the polarization direction. Thus if the waves have different polarization directions, it is often possible to find a propagation direction along which phase matching is achieved.

The second method is called Quasi-phase matching (QPM)³. With no phase matching, maximum amplitude of the generated wave is reached after a distance l_{coh} where $\Delta k \cdot l_{coh} = \pi$. After this distance, known as coherence length, the amplitude starts to decrease because of destructive interference. But if the crystal orientation is altered, and the sign of the nonlinear coefficient is reversed, so that the next component of the generated wave is added with an additional π phase shift, then the constructive addition continues and the generated wave continues to grow. The technique for creating this kind of periodical domain inversion is known as periodic poling. The advantages of the QPM method are that phase matching can be achieved at any wavelength within the transparency range of the nonlinear material by choosing the correct period of the domain inversion, and that the largest nonlinear coefficient can be utilized. These periodically poled materials have been widely used for generating infrared light. But for generating the visible light, the domain periods required are typically between 4 μm and 7 μm ,

which are much smaller than that for the infrared, and are more difficult to fabricate repeatedly⁴. Thus for visible light generation, periodically poled nonlinear materials are still currently under development, so bulk crystals are still the main choice.

Continuous wave second harmonic generation

Second harmonic generation is the simplest and most familiar nonlinear interaction. The first experiment "that ushered in the field of nonlinear optics"¹ was done in 1961 by Franken et al.⁵. The early experiments were done with pulsed lasers, and the pulsed SHG could yield very high conversion efficiency (close to 100%) and a high average power⁶, due to the high peak power of the pulsed laser.

For CW operation, single-pass conversion efficiency is relatively low because of the lack of high power. Resonant enhancement by an optical cavity can be used to improve the efficiency. The high circulating fundamental light plus the small beam size created by the cavity configuration can result in a high focused intensity, and therefore a high conversion efficiency. If the nonlinear crystal is placed into the same cavity with the laser gain medium, this method is called intracavity frequency doubling. Many commercial green light sources at 532nm use this method, with high efficiency over 60% and high CW power (over 10W is not uncommon).

To double a monolithic laser, such as a diode laser, the nonlinear crystal is placed in an external cavity, which is known as extracavity frequency doubling. The conversion efficiency of doubling solid-state lasers or gas lasers can reach more than 80%. For example, the highest conversion efficiency is 89% for doubling the Nd:YAG laser at

1.06 μm , and the output power of the second harmonic (SH) light more than is 1W⁷.

Solid-state lasers, such as the Nd:YAG usually have relatively high powers with good spatial and spectral properties. The overall conversion efficiency of the laser is relatively low, usually within a few percents, and the wavelength tuning is limited.

Direct frequency doubling a diode laser is more attractive and can benefit from many of the desired characteristics of the diode laser. These benefits include: high efficiency, compact size, low cost, a large wavelength tuning range, etc. The efficiency of direct frequency doubling a diode laser is lower than that of doubling a solid-state laser; for example, the conversion efficiency is about 40% using a monolithic cavity⁸. Using a master oscillation passive amplification (MOPA) laser, which has a much higher output power, the efficiency can reach 58% with 1W of harmonic light⁹. In Table-1, some CW SHG experiments are listed; the conversion efficiencies are calculated with coupled fundamental power. The optical-optical efficiencies, which are calculated with the total output pump power, are lower. One of the reasons for the lowered conversion efficiency is that because of the elliptical output beam shape of laser diode, mode matching to the external resonant cavity is usually low. Using an anamorphic prism pair to change the ellipticity and other optics costs additional loss of the pump light.

For efficient SHG, the diode laser must be single longitudinal mode with a narrow linewidth, such as a distributed Bragg deflector (DBR) laser, a distributed feedback (DFB) laser or an external-cavity diode laser (ECDL). However, these are relatively expensive and sometimes difficult to obtain in the desired wavelength range, especially with high powers. As an alternative, high power Fabry-Perot diode lasers are much less

expensive and easily obtainable, although these lasers are usually multimode and the linewidth of the individual modes is large (several tens to hundreds megahertz). The difficulty becomes how to achieve stable single mode operation and a narrow linewidth without losing a significant amount of the output power. One approach to narrow the linewidth is passive locking, in which the transmission from an external high-finesse cavity is fed back to the diode laser¹⁰. When the frequency of the of single-mode free-running diode laser is close to the cavity resonance, the laser frequency will jump to the resonance and the linewidth is also reduced by up to three orders of magnitude. For a multimode laser, to obtain single mode operation, the transmission of the external resonant cavity is fed back into the laser after reflecting off a grating. Besides the diode laser operating in a single mode, the diode laser self-locks to the ring cavity resonance.

This thesis will describe a blue light source by frequency doubling a Fabry-Perot diode laser in an external ring cavity using both cavity and grating feedback^{11,12}.

Overview of the thesis

This thesis is organized in four chapters. In this first chapter we have presented a short background of SHG. The external resonant cavity plays a significant role in SHG, and the efficiency depends on the mode matching, so the mode matching between the diode laser and the ring cavity is discussed in Chapter-2. In Chapter-3, the SHG is calculated using the Fourier-space method. Chapter-4 describes our blue light source by frequency doubling an infrared diode laser, and the experimental results are compared with the simulation in Chapter-3.

Table -1.1 CW SHG Experiments

Wavelength (nm)	Pump & Power	Nonlinear Crystal	Cavity	SH Power	Conversion efficiency	Reference
473	Nd:YAG 1.1W	KNbO ₃ 5 mm	Semi-monolithic	500 mW	>81%	13
532	Miniature Nd:YAG 1.64 W	MgO:LiNbO ₃ 7.5 mm	Semi-monolithic	1.1 W	89%	7
532	Nd:YAG 175 mW	MgO:LiNbO ₃ 7.5mm	Standing wave monolithic	130 mW	82%	14
532	Ar ⁺ laser 1 W	MgO:LiNbO ₃ 7.5 mm	Ring	0.5 W	70%	15
540	Nd:YAG 0.7W	KTP 10mm	Ring	560 mW	85%	16
266	Intracavity doubled Nd:YVO ₄ 500mW	BBO 12mm	Ring	100mW	22%	17
532	Nd:YAG 6.5 W	Periodically poled LiNbO ₃ 53mm	Single pass	2.7 W	42%	18
427	External-cavity diode laser 70 mW	KNbO ₃ 9mm	Ring	7.8 mW	34%	19
429	AR- coated Diode laser 80mW	KNbO ₃ 6mm	Monolithic ring	14 mW	20%	20
428	Single mode diode 160 mW	KNbO ₃ 6mm	Monolithic ring	41 mW	40%	8
465	MOPA 4W	LBO 4 mm	Ring	1W	58%	9
390	External-cavity tapered diode 1W	BBO 18mm	ring	233 mW	39%	21
403	MOPA 400mW	LBO 16mm	Ring	98 mW	25%	22
486	MOPA 740mW	KNbO ₃ 6.5mm	Ring	156 mW	40%	23
532	α-DFB 350mW	KTP 10mm	Ring	120 mW	34%	24
421	Single mode diode 100mW	KNBO ₃ 5mm	Ring	6.7mW	11%	25
392	External-cavity tapered diode 1W	BBO 5mm	Ring	100mW	20%	26

CHAPTER 2

BOW TIE RING CAVITY DESIGN

Bow tie ring cavities are often chosen for the external resonant field enhancement in extracavity frequency conversion experiments. The ring cavity, illustrated in Figure-2.2.1, consists of two plane mirrors M1 and M2, and two curved mirrors M3 and M4. The stable cavity mode has two beam waists: a smaller beam waist located in the center between the two spherical mirrors, where the nonlinear crystal is placed, and a larger elliptical beam waist located between the two plane mirrors. Typically the diode laser output is focused into the larger elliptical beam waist for mode matching.

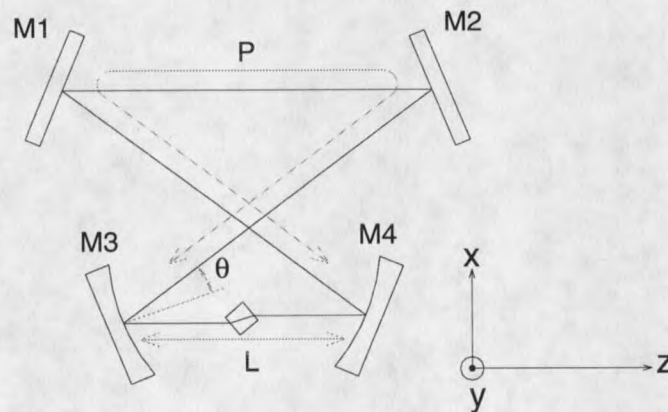


Figure-2.1 The bow tie ring cavity is formed by two plane mirrors (M1 and M2) and two spherical mirrors (M3 and M4). The incident angles on the cavity mirrors are θ , the distance between the two spherical mirrors (M3-M4) is L , and the distance between the two spherical mirrors via plane mirrors (M4-M1-M2-M3) is P .

The ring cavity has two main advantages. First, there is no direct reflection from the cavity optics back towards the diode laser so that destructive optical feedback can be

avoided. Second, a uni-directional traveling harmonic wave is produced inside the cavity, which is convenient for output coupling.

Mode in a bow tie ring cavity

To maximize the efficiency of the frequency doubling, knowledge of the exact beam waist size and location inside the crystal is necessary²⁷. Such analysis is usually carried out using the ABCD law and the self-consistency postulate^{28,29}.

Usually the bow tie ring cavity will be symmetric, with θ being the incident angle of the beam on the curved mirrors, and R the radius of the curved mirrors. As illustrated in Figure-2.1, the distance between the two curved mirrors is L , while the distance between the two curved mirrors via the two plane mirrors is P . Thus the total cavity path length is $L + P$. The complex beam parameter $q(z)$ at position z in the cavity is determined by the ABCD law for the resonator and the self-consistency postulate^{2,3}:

$$q(z) = \frac{A(z)q(z) + B(z)}{C(z)q(z) + D(z)} \quad 2.1$$

where A, B, C and D are the components of the ABCD matrix that describes one complete round-trip inside the cavity. The roots of the resulting quadratic equation of Equation-2.1 are:

$$\frac{1}{q(z)} = \frac{D - A}{2B} \pm \frac{i}{2B} \sqrt{-(A - D)^2 + 4BC} \quad 2.2$$

Without the crystal inside the ring cavity, the ABCD matrix for a point at distance z_1 from M4, can be expressed as:

$$\begin{bmatrix} A & B \\ C & D \end{bmatrix} = \begin{bmatrix} \frac{f_e^2 - f_e(2z_1 + P) + z_1 P}{f_e^2} & \frac{f_e^2(z_1 + z_2 + P) - f_e[z_1(2z_2 + P) + z_2 P] + z_1 z_2 P}{f_e^2} \\ \frac{P - 2f_e}{f_e^2} & \frac{f_e^2 - f_e(2z_2 + P) + z_2 P}{f_e^2} \end{bmatrix} \quad 2.3$$

where $z_2 = L - z_1$, and f_e represents the effective focal length for the horizontal plane f_x or that for the vertical plane f_y .

At the beam waist, $\frac{1}{q(z)}$ is a pure imaginary number, so $D = A$. Using the expression for D and A from Equation-2.3, yields $z_1 = z_2$, which means the beam waist is at the center between the two curved mirrors. This is consistent with the symmetry of the cavity. With $z_1 = z_2 = L/2$, the beam radius ω is:

$$\omega^2 = \frac{\lambda}{2\pi} \sqrt{\frac{4f_e^2(L+P) - 2f_e \cdot L \cdot (L+2P) + L^2 P}{P - 2f_e}} \quad 2.4$$

It is well known that a spherical mirror used at oblique incidence focuses vertical plane ray bundles at a different location than horizontal plane ray bundles. This is manifested in two different effective focal lengths f_y and f_x , where³⁰

$$\begin{aligned} f_y &= \frac{f}{\cos \theta} \\ f_x &= f \cos \theta \end{aligned} \quad 2.5$$

with $f = R/2$.

With equation-2.4 and 2.5, the beam waists for the horizontal plane and the vertical plane are:

$$\omega_{0x}^2 = \frac{\lambda \cdot f}{2 \cdot \pi} \cdot \sqrt{\frac{l - 2 \cdot \cos \theta}{p - 2 \cdot \cos \theta}} \cdot [2 \cdot (l + p) \cdot \cos \theta - l \cdot p] \quad 2.6a$$

$$\omega_{0y}^2 = \frac{\lambda \cdot f}{2 \cdot \pi} \cdot \sqrt{\frac{l \cdot \cos \theta - 2}{\cos \theta \cdot (p \cdot \cos \theta - 2)}} \cdot [2 \cdot (l + p) - l \cdot p \cdot \cos \theta] \quad 2.6b$$

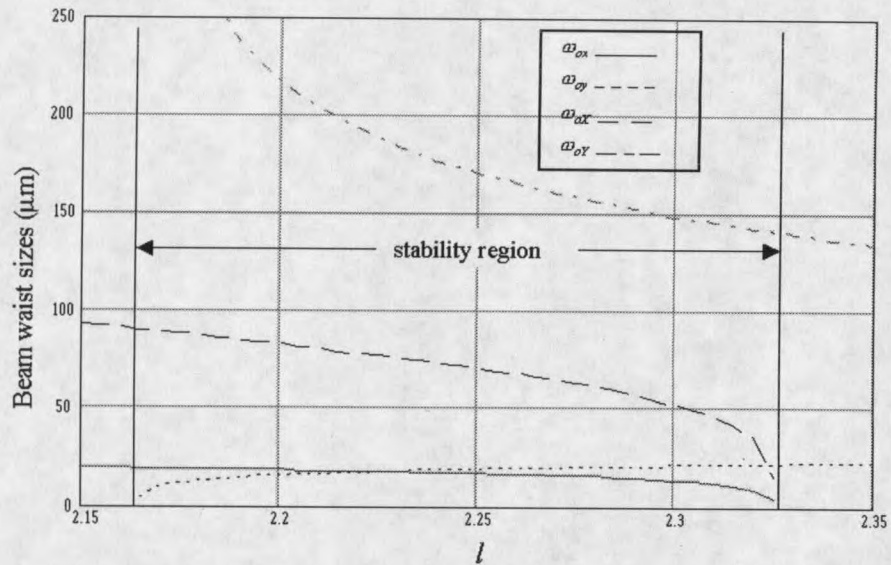
Here $l = \frac{L}{f}$ and $p = \frac{P}{f}$, so that L and P are normalized to f .

By using Gaussian beam propagation through a thin lens, we found that the second beam waists for the horizontal and vertical planes are located at the center of the plane mirrors, and the sizes are:

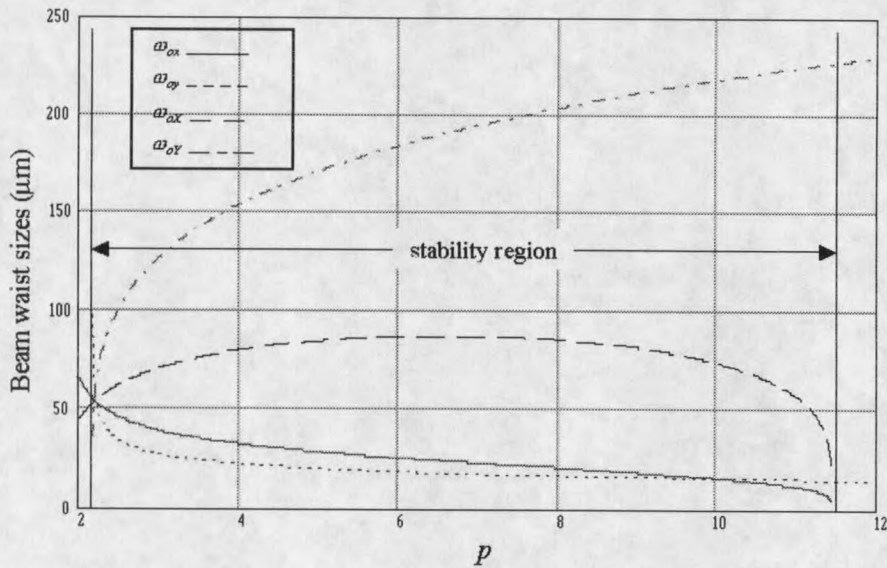
$$\omega_{0x}^2 = \frac{\lambda \cdot f}{2 \cdot \pi} \cdot \sqrt{\frac{p - 2 \cdot \cos \theta}{l - 2 \cdot \cos \theta}} \cdot [2 \cdot (l + p) \cdot \cos \theta - l \cdot p] \quad 2.7a$$

$$\omega_{0y}^2 = \frac{\lambda \cdot f}{2 \cdot \pi} \cdot \sqrt{\frac{p \cdot \cos \theta - 2}{\cos \theta \cdot (l \cdot \cos \theta - 2)}} \cdot [2 \cdot (l + p) - l \cdot p \cdot \cos \theta] \quad 2.7b$$

Comparison of Equations 2.6 and 2.7 reveals that the result is just the exchange of l and p ; this is also consistent with the structure of the cavity. In Figure-2.2 we plot the calculated beam waists in the ring cavity as a function of mirror separation p and l . We can see from the plot that ω_{0x} and ω_{0y} are generally smaller than ω_{0x} and ω_{0y} , and the large beam waist is elliptical. By choosing the parameters l , p and θ , we can make the small beam waist circular. The sizes of the cavity beam waist are proportional to \sqrt{R} as shown in Equation 2.6 and 2.7.



(a)



(b)

Figure-2.2 The calculated beam waists in the ring cavity as a function of mirror separation p and l using equation 2.6 and 2.7. The parameters used here are: wavelength $\lambda = 1\mu\text{m}$, radius of M3 and M4 $R = 20\text{mm}$ and angle of incidence $\theta = 22.5^\circ$. (a) As a function of l , with $p = 9.0$. (b) As a function of p , with $l = 2.2$. The stability region will be discussed in the next section.

